# Extracellular Release of ILEI/FAM3C and Amyloid-β is Associated with the Activation of Distinct Synapse Subpopulations

Masaki Nakano[a], Yachiyo Mitsuishi[a], Lei Liu[a,b], Naoki Watanabe[a], Emi Hibino[a], Saori Hata[c,d], Takashi Saito[e,f], Takaomi C Saido[e], Shigeo Murayama[g,h], Kensaku Kasuga[i], Takeshi Ikeuchi[i], Toshiharu Suzuki[c], Masaki Nishimura[a*]

Running title: Distinct activity-dependent secretion of ILEI and Aβ

[a] Molecular Neuroscience Research Center, Shiga University of Medical Science, Shiga, 520-2192, Japan

[b] Present address: Ann Romney Center for Neurologic Diseases, Brigham and Women's Hospital, Harvard Medical School, Boston, MA, 02115, USA

[c] Laboratory of Neuroscience, Graduate School of Pharmaceutical Sciences, Hokkaido University, Hokkaido, 060-0812, Japan

[d] Biomedical Research Institute, National Institute of Advanced Industrial Science and Technology (AIST), Tsukuba, 305-8566, Japan

[e] Laboratory for Proteolytic Neuroscience, RIKEN Brain Science Institute, Saitama, 351-0198, Japan

[f] Department of Neurocognitive Science, Institute of Brain Science, Nagoya City University Graduate School of Medical Science, Nagoya, 467-8196, Japan

[g] Department of Neurology and Neuropathology (the Brain Bank for Aging Research), Tokyo Metropolitan Geriatric Hospital and Institute of Gerontology, Tokyo, 173-0015, Japan

[h] Present address: Brain Bank for Neurodevelopmental, Neurological and Psychiatric Disorders, United Graduate School of Child, Development, Osaka University, Osaka, 565-0871, Japan

[i] Department of Molecular Genetics, Brain Research Institute, Niigata University, Niigata, 951-8585, Japan

Correspondence to: Masaki Nishimura, Molecular Neuroscience Research Center, Shiga University of Medical Science, Shiga, 520-2192, Japan, Tel: +81-77-548-2328, Fax: +81-77-548-2210; E-mail: mnishimu@belle.shiga-med.ac.jp.

Total number of words: 7,698

**Abstract**

**Background:** Brain amyloid-β (Aβ) peptide is released into the interstitial fluid (ISF) in a neuronal activity-dependent manner, and Aβ deposition in Alzheimer's disease (AD) is linked to baseline neuronal activity. Although the intrinsic mechanism for Aβ generation remains to be elucidated, interleukin-like epithelial-mesenchymal transition inducer (ILEI) is a candidate for an endogenous Aβ suppressor.

**Objective:** This study aimed to access the mechanism underlying ILEI secretion and its effect on Aβ production in the brain.

**Methods:** ILEI and Aβ levels in the cerebral cortex were monitored using a newly developed ILEI-specific ELISA and *in vivo* microdialysis in mutant human Aβ precursor protein-knockin mice. ILEI levels in autopsied brains and cerebrospinal fluid (CSF) were measured using ELISA.

**Results:** Extracellular release of ILEI and Aβ was dependent on neuronal activation and specifically on tetanus toxin-sensitive exocytosis of synaptic vesicles. However, simultaneous monitoring of extracellular ILEI and Aβ revealed that a spontaneous fluctuation of ILEI levels appeared to inversely mirror that of Aβ levels. Selective activation and inhibition of synaptic receptors differentially altered these levels. The evoked activation of AMPA-type receptors resulted in opposing changes to ILEI and Aβ levels. Brain ILEI levels were selectively decreased in AD. CSF ILEI concentration correlated with that of Aβ, and were reduced in AD and mild cognitive impairment.

**Conclusion:** ILEI and Aβ are released from distinct subpopulations of synaptic terminals in an activity-dependent manner, and ILEI negatively regulates Aβ production in specific synapse types. CSF ILEI might represent a surrogate marker for the accumulation of brain Aβ.

**Keywords:** Alzheimer's disease, Aβ, ILEI, Synapse, Neurotransmitter receptor

## INTRODUCTION

Family with sequence similarity 3, member C (FAM3C) is a ubiquitously expressed, multi-functional secretory protein. It is upregulated by transforming growth factor β signaling and causes epithelial-mesenchymal transition of epithelial cells and hepatocytes; thus, FAM3C has also been named interleukin-like epithelial-mesenchymal transition inducer (ILEI) [1-5]. Other emerging functions of FAM3C/ILEI include inhibition of osteoblast differentiation and mineralization through Runx2 downregulation in the bone marrow [6, 7], and gluconeogenesis suppression via induction of heat shock factor 1, and activation of the phosphoinositide 3-kinase and Akt pathway in the liver [8, 9].

In previous studies, we found that extracellularly released ILEI interacts with the γ-secretase complex to suppress production of amyloid-β (Aβ) peptides [10]. Aβ is generated through β- and γ-secretase-mediated proteolytic processing of Aβ precursor protein (AβPP) and is released into the interstitial fluid (ISF) of brain parenchyma in a neuronal activity-dependent manner [11, 12]. Excessive accumulation of aggregated Aβ in the cerebral cortex and hippocampus is considered to initiate the pathogenic cascade of Alzheimer's disease (AD). Recent imaging studies revealed that Aβ deposition in the brain is tightly linked to baseline neuronal activity, and that component regions of the default mode network are the sites most vulnerable to Aβ deposition [13, 14]. ILEI reduces Aβ production by facilitating lysosome/proteasome-mediated turnover of the C-terminal fragments of AβPP while sparing γ-secretase activity. During AD pathogenesis, the expression of ILEI is significantly reduced in the brain and inversely correlated with accumulated Aβ levels [10, 15]. These findings suggest that reduced

74 expression of brain ILEI is an antecedent event that prompts the inevitable Aβ pathology observed in
75 AD.

76 We previously reported that ILEI colocalizes with AβPP and γ-secretase complex components
77 at the presynaptic terminals [15]. However, two questions remain unanswered: (1) how is ILEI released
78 into the ISF and (2) is there a relationship between extracellularly released ILEI and Aβ levels? In this
79 study, we developed a sandwich ELISA for ILEI that enabled quantitative analysis of expression and
80 secretion of ILEI in the mouse brain. Using *in vivo* microdialysis, we found that ILEI was released into
81 the ISF in a neuronal activity-dependent manner, much like Aβ. Moreover, activation or inhibition of
82 specific neurotransmitter receptors led to distinct changes in the extracellular levels of ILEI and Aβ in
83 the cerebral cortex.

84

85 **MATERIALS AND METHODS**

86 *Preparation of monoclonal antibodies against ILEI*

87 To generate monoclonal antibodies against ILEI protein, two BDF1 mice were immunized with a
88 recombinant His-tagged, secreted form of human ILEI (25-227 amino acid residues, #ATGP1251,
89 ATGen Co. Ltd., Gyeonggi-do, Korea). After preparation of the lymph nodes and spleens, cells were
90 fused with the myeloma cell line P3-X63-Ag8. The hybridoma supernatants of mixed clones were
91 screened by ELISA. Among 95 clones that recognized the immunogen, three monoclonal antibody
92 clones showed the highest immunoreactivity after the second round of subcloning by limiting dilution.

93 Finally, two clones, namely 24C1 and 42C1, were selected by ELISA against recombinant mouse ILEI
94 (R&D Systems Inc., Minneapolis, MN, Cat# 2868-FM). Both monoclonal antibodies were purified by
95 protein A affinity chromatography from 1 L of each hybridoma cell culture supernatant. In addition, the
96 antibody mAb24C1 was conjugated to horseradish peroxidase according to the manufacturer's
97 instructions (Dojindo, Kumamoto, Japan, Cat# LK11).
98
99 *Development of a sandwich ELISA for ILEI*
100 First, 96-well flat-bottom ELISA plates (Nunc, Thermo Fisher Scientific, Rochester, NY, Cat# 469914)
101 were coated with mAb42C1 (144 ng/well in 100 μL/well of 0.2 M sodium carbonate–bicarbonate buffer,
102 pH 9.4). The plates were incubated at 4°C overnight and then washed three times with 300 μL/well of
103 PBS (pH 7.2) with 0.1% Tween 20. Nonspecific binding sites were blocked by incubation with a
104 blocking reagent (IS-CD-500E; Cosmo Bio. Co, Ltd., Tokyo, Japan, Cat# IS-CD-500E) for 1 h at 37°C.
105 The standards were prepared with a solution of recombinant mouse ILEI (2868-FM; R&D
106 system, Inc., Cat# 2868-FM) or human ILEI (15678-H08H-50, Sino Biological Inc., Beijing, China,
107 Cat# 15678-H08H-50) in a dilution buffer (Immuno-Biological Laboratories Co, Ltd., Gunma, Japan,
108 Cat# 27769D100). Standards of 0.313, 0.625, 1.25, 2.5, 5.0, and 10.0 ng/mL were prepared immediately
109 before loading. Unknown samples were prepared in an appropriate dilution with dilution buffer. Wells
110 were each loaded with 100 μL of the designated solution. The plates were subsequently incubated for 18
111 h at 4°C without shaking before being washed five times.

The plates were then incubated with the detection antibody solution, which contained horseradish-peroxidase-conjugated antibody mAb24C1 at 50 ng/well in 100 μL/well of a dilution buffer (Immuno Shot 2; Cosmo Bio, Cat# IS-002) for 1 h at 4°C. They were then washed five times, incubated for another hour at room temperature, and again washed five times. Subsequently, the plates were developed for 30 min with 100 μL/well of a 3,3',5,5'-tetramethylbenzidine dihydrochloride substrate solution (ImmunoPure Turbo TMB; Pierce Chemical Co., Rockford, IL, Cat# 5120). The reaction was stopped by adding 100 μL/well of 1 M sulfuric acid (Nacalai Tesque, Kyoto, Japan, Cat# 95626-06). Finally, the plates were read at a wavelength of 450 nm (Benchmark Plus; Bio-Rad Laboratories Inc., Hercules, CA, USA).

*Immunoblotting*

ILEI-knockout HEK293 cells [15] were transfected with expression plasmids using linear polyethylenimine (Polysciences Inc., Warrington, PA, Cat# 23966). Cell lysates were sonicated on ice and centrifuged at 4°C and 15,000 rpm for 25 min. Per lane, 15–20 μg of proteins were separated by 12% SDS-PAGE and transferred to a polyvinylidene fluoride membrane (Merck Millipore, Co., Billerica, MA, Cat# IPVH00010). These membranes were incubated with the primary antibodies at 4°C overnight before being washed and incubated with corresponding horseradish peroxidase-conjugated secondary antibodies (1:5,000, Merck Millipore, Cat# AP308P) for 1 h. This process was followed by enhanced chemiluminescence detection (Nacalai Tesque, Cat# 07880-70). Blots were scanned using a

LAS-4000 imaging system (Fujifilm, Tokyo, Japan). The primary antibodies used were as follows: mAb42C1 (1:2,000), mAb24C1 (1:2,000), anti-GAPDH antibody (1:2,000, Merck Millipore, Cat# MAB2549), and anti-V5 antibody (1:2,000, Nacalai Tesque, Cat# 04434-94).

*Animals*

Four month-old male C57BL/6J mice (CLEA Japan, Inc., Tokyo, Japan) and humanized mutant AβPP-knockin mice ($App^{NL-G-F}$ mice [16]) were used in this study. Mice were maintained at room temperature (25°C) under a standard 12:12 h light:dark cycle, with food and water available *ad libitum*. $App^{NL-G-F}$ mice were intraperitoneally injected with a mixture of anesthetics (Domitor, ZENOAQ, Fukushima, Japan; Vetorphale, Meiji Seika Pharma Co., Ltd., Tokyo, Japan; midazolam, Sando Co., Ltd., Tokyo, Japan) and then with an anti-anesthetic (Antisedan, ZENOAQ, Fukushima, Japan). Tetanus toxin (Sigma, St. Louis, MO, Cat# T3194) was also intraperitoneally administered. All experimental procedures were approved by the Institutional Animal Care and Use Committee of the Shiga University of Medical Science (Approval ID: 2018-12-1), and experiments were performed according to the Guide for the Care and Use of Laboratory Animals.

*Measurement of ILEI and Aβ in the mouse brain*

Mice were euthanized by cervical dislocation, and whole brains and cerebrospinal fluid (CSF) were obtained. Whole forebrains were homogenized using a motor-driven Teflon/glass homogenizer (10

150 strokes) in four volumes of Tris-buffered saline (50 mM Tris, pH 7.6, 150 mM NaCl, and 0.5 mM
151 EDTA) that contained a protease inhibitor cocktail. The homogenates were then centrifuged at 100,000
152 *g* for 20 min on a TLA 100.4 rotor in a TLX ultracentrifuge (Beckman, Palo Alto, CA, USA). The
153 supernatants were taken as the soluble fractions and subjected to a protein assay (BioRad, Cat# 500-
154 0116JA) and sandwich ELISAs specific for ILEI, mouse/rat Aβ40 (Immuno-Biological Laboratories,
155 Cat# 27720), or human total Aβ (Immuno-Biological Laboratories, Cat# 27729). Brain lysates were
156 obtained by adding NP40 and CHAPSO to homogenates at 1% of each final concentration.
157
158 *In vivo microdialysis*
159 Microdialysis was performed as previously described by Takeda et al. [17]. Briefly, guide cannulas (8
160 mm in length) were stereotactically implanted into the right cerebral cortex (bregma 1.9 mm, 0.5 mm
161 lateral to the midline, and 0.8 mm ventral to skull surface) of anesthetized mice, and then bonded in place
162 with dental cement. Accordingly, the inserted dialysis probe was located in the medial prefrontal cortex
163 spanning the anterior cingulate, prelimbic, and infralimbic areas, which are AD-vulnerable regions. At
164 least two days after guide cannula implantation, a microdialysis probe with a 2 mm-long polyethylene
165 membrane (1,000 kDa molecular weight cutoff, PEP-4-02, Eicom, Kyoto, Japan, Cat# 600132) was
166 inserted through the guide, and the mouse was placed in a transparent acrylic cage (250 × 250 × 350
167 (height) mm). The probe was connected to peristaltic and microsyringe pumps with fluorinated ethylene
168 propylene tubing (250 μm in diameter): the syringe pump pushed and the peristaltic pump pulled a

dialysis buffer (119 mM NaCl, 2.5 mM KCl, 2.5 mM $CaCl_2$, and 0.15% bovine serum albumin; filtered through a 0.22-μm-pore-sized membrane) at a synchronous flow rate. After preperfusion with a dialysis buffer at a flow rate of 10 μL/min for 2 h, dialyzed samples were collected into polypropylene tubes every 1 or 2 h using a fraction collector (EFC-96, Eicom). During sampling, flow rate was kept constant at 0.5 μL/min. Sampling began at 16:00, and the mice were allowed to move freely in the cage while sampling occurred. The concentrations of ILEI and Aβ were measured using the ELISAs described above. Basal levels of ILEI or Aβ were defined as the mean concentration from four samples obtained before reverse dialysis. All values for each mouse were then normalized as percentages of the basal level for each point.

*Assessment of mouse locomotor activity*

To assess mouse locomotor activity during microdialysis, we used the Scanet MV-40 system (Melquest, Toyama, Japan). Vertical and horizontal movements of mice were tracked and measured every 60 min for 2 days using digital counters with infrared sensors, which were crosswise distributed at 6-mm intervals and a height of 30 mm above the floor of a transparent acrylic cage (250 × 250 mm). The moving distances of mice every hour were expressed in arbitrary units.

*Reverse microdialysis*

187 The following compounds were used for reverse microdialysis: tetrodotoxin (Fujifilm Wako, Tokyo,
188 Japan, Cat# 206-11071), AMPA (Abcam, Cambridge, UK, Cat# ab12005), NBQX disodium salt
189 (Abcam, Cat# ab144489), NMDA (Nacalai Tesque, Cat# 22034-16), D-AP5 (Abcam, Cat# ab120003),
190 diazepam (Fujifilm Wako, Cat# 045-18901), picrotoxin (Sigma Chemicals, Cat# P1675), (R, S)-
191 Baclofen (Abcam, Cat# ab120149), CGP55845 hydrochloride (Sigma Chemicals, Cat# SML0594),
192 nicotine (Nacalai Tesque, Cat# 24332-62), D-tubocurarine chloride (Nacalai Tesque, Cat# 35637-84),
193 pilocarpine hydrochloride (Nacalai Tesque, Cat# 28008-31), and atropine sulfate (Nacalai Tesque, Cat#
194 03533-11). For reverse microdialysis, compounds were diluted at the indicated concentration in Ringer's
195 solution.
196
197 *Autopsied human brain tissues*
198 Frozen brain tissues from the temporal cortex of 15 deceased patients with AD, 15 age-matched non-
199 neurological disease control subjects, and 10 non-AD neurological disease control subjects were
200 obtained from the Brain Bank for Aging Research, Tokyo Metropolitan Institute of Gerontology (Tokyo,
201 Japan). All study subjects or their next of kin provided written informed consent for brain donation, and
202 experimental procedures were approved by the Shiga University of Medical Science Review Board
203 (Approval ID: 28-096). All patients with AD fulfilled the National Institute of Neurological and
204 Communicative Disorders and Stroke-Alzheimer's Disease and Related Disorders Associations criteria

for probable AD. Soluble fractions of temporal cortex homogenates were prepared as previously described (10).

*Clinical CSF samples*

CSF was analyzed in control subjects (mean age 76.88 years, n = 25), MCI subjects (mean age 71.24 years, n = 25), and patients with AD (mean age 75.84 years, n = 25). Written informed consent was obtained from each participant before lumbar puncture for CSF collection. CSF analysis was approved by the Ethics Committees of Niigata University (Approval ID: 2015-2427). CSF concentrations of $A\beta_{38}$, $A\beta_{40}$, and $A\beta_{42}$ were analyzed using V-PLEX Aβ Peptide Panel 1 (6E10) (Meso Scale Discovery, Rockville, MD) with MESO QuickPlex SQ 120 (Meso Scale Diagnostics). Intra- and interassay coefficients of variation were <20% for all assays. The ILEI measurement of CSF samples was approved by the Ethics Committees of Shiga University of Medical Science (Approval ID: 27-210).

*Statistical analysis*

Statistical analyses involved two-tailed unpaired Student's *t*-tests or one-way ANOVA combined with Dunnett's test for multiple comparisons. Correlation analyses were performed using the Spearman's rank correlation test. StatPlus:mac LE software (AnalystSoft, Vancouver, Canada) was used for statistical analyses. All data are presented as means ± SEMs. $P$ values < 0.05 were considered to be statistically significant.

## RESULTS

*Monoclonal antibodies 24C1 and 42C1 recognize distinct epitopes of ILEI protein*

We generated monoclonal antibodies against ILEI by immunizing BDF1 mice with recombinant His-tagged, human ILEI that was purified from conditioned medium of ILEI-overexpressing HEK293 cells. Based on immunoblotting of HEK293 cell lysate and ELISA against recombinant ILEI, we selected the clones 24C1 and 42C1. The monoclonal antibodies mAb24C1 and mAb42C1 recognized both human and mouse ILEI proteins according to immunoblotting and ELISA.

To define each epitope of these antibodies, we first generated expression vectors for human ILEI mutants harboring deletion or truncation of amino acid residues 25–99 (Δ25–99), 100–154 (Δ100–154), 155–190 (Δ155–190), or 191–227 (Δ191–227) (Fig. 1A). Immunoblotting of mutant ILEI-transfected HEK293 cell lysates revealed that mAb24C1 failed to label ILEI-Δ155–190, whereas mAb42C1 did not react with ILEI-Δ191–227 (Fig. 1B). We also prepared several missense ILEI mutants harboring alanine substitutions of evolutionally conserved amino acid residues: G103A, G169A, D151A, R179A, W212A, C58A, C64A, C86A, and C221A. Immunoblotting revealed that mAb24C1 and mAb42C1 selectively lacked immunoreactivity to G169A-ILEI and W212A-ILEI, respectively (Fig. 1C). According to a previous report on crystal structure [18], $Gly^{169}$ and $Trp^{212}$ are surface-exposed and distant from each other in their respective locations (Fig. 1D). These results suggest that mAb24C1 and

mAb42C1 recognize distinct epitopes of ILEI, to which the residues $Gly^{169}$ and $Trp^{212}$ are critical, respectively.

*Development and validation of the ILEI-specific ELISA*

In our sandwich ELISA that was specific for ILEI, mAb42C1 was suitable as a capture antibody and horseradish peroxidase-labeled mAb24C1 was useful as a detection antibody. The optimized concentrations of the capture and detection antibodies were 1.44 and 0.50 μg/mL, respectively. The performance of this ELISA for recombinant mouse and human ILEI are shown in Fig. 1E. The standard curves were based on six serial dilutions of mouse or human recombinant ILEI and were linear over 0.31–10.0 ng/mL. The detection limit (3.3 s/a, where s = SD of the blank; a = slope of the standard curve) and the quantification limit (10 s/a), which were based on eight independent determinations of a blank in standard solutions, were 0.04 and 0.11 ng/mL for mouse ILEI, respectively, and 0.05 and 0.16 ng/mL for human ILEI, respectively.

For validation of the assay at different dilutions, we used soluble fractions of mouse brain homogenates diluted at 1:10. Dilutional parallelism was determined by evaluating each sample at its initial strength (1:10) and at dilutions of 1:2, 1:4, and 1:8. Observed-to-expected ratios for the dilutional parallelism of each sample of the full-strength solution ranged from 85% to 136%. Spiking recovery was determined by adding 0.0, 1.25, 2.50, and 5.00 ng/mL of recombinant ILEI to mouse brain homogenate samples. Observed-to-expected ratios for spiking recovery of the homogenate diluted at 1:40 ranged

261 from 88% to 89%. The intra-assay coefficient of variation for soluble fractions of brain homogenates
262 was <10%.

263 A study reported homodimerization of ILEI via intermolecular disulfide bonds [18]. According
264 to the predicted conformation of dimerized ILEI [18], mAb42C1 recognized the opposite side of the
265 binding interface, whereas the recognition site of mAb24C1 may be occluded by the binding interface.
266 Both antibodies detected a single band corresponding to monomer ILEI in mouse brain lysates under
267 reducing or nonreducing conditions (Fig. 1F). The nonreduced ILEI monomer migrated faster in SDS-
268 PAGE than the disulfide-reduced ILEI monomer (Fig. 1F), which can be explained by the formation of
269 intramolecular disulfide bonds [18]. This indicated that no detectable level of ILEI homodimer was
270 present in the mouse brain, at least using these antibodies.

271

272 *Expression and secretion of ILEI in the mouse forebrain*

273 We collected brains and CSF every 3 h for 24 h from C57BL/6J mice housed under a 12:12 h
274 light:dark cycle and then measured ILEI levels using the established ELISA. To examine expression
275 levels of brain ILEI, we prepared NP40- and CHAPSO-solubilized lysates of forebrains. ILEI
276 concentrations of forebrain lysates were within a relatively narrow range during day/night cycles (Fig.
277 2A). To assess secretion of ILEI, we used the supernatant from ultracentrifuged forebrain homogenates.
278 The ILEI concentrations of the soluble fractions changed periodically (Fig. 2B); thus, the extracellular

279 release of ILEI apparently fluctuated over time. The levels of CSF ILEI also fluctuated but were not
280 synchronized with levels of ILEI in the soluble brain fractions (Fig. 2C).

281 Furthermore, we measured Aβ concentrations in these same samples. Aβ levels showed
282 fluctuations that were more prominent in the soluble fractions than in the lysates and were not associated
283 with the fluctuations of ILEI levels (Fig. 2D, E). However, Aβ fluctuation was roughly parallel to ILEI
284 fluctuation in the CSF (Fig. 2F).

285

286 *Monitoring of cortical ISF ILEI and Aβ by in vivo microdialysis*

287 We used *in vivo* microdialysis to monitor ISF ILEI and Aβ in the cerebral cortex of conscious,
288 freely-moving $App^{NL-G-F}$ knockin (KI) mice (3–4-months old), in which the humanized mutant AβPP is
289 expressed under its endogenous promoter [16]. Dialysates were collected every hour and mouse
290 movement was tracked. Levels of ISF ILEI periodically fluctuated and higher levels were weakly
291 associated with higher locomotor activity (Fig. 3A, B). Intraperitoneally injected anesthetics suppressed
292 ILEI levels in the dialysates; however, these levels were restored by treatment with an anti-anesthetic
293 (Fig. 3C). Anesthetic treatment also decreased Aβ levels with kinetics that were similar to ILEI levels
294 (Fig. 3D). Although ISF Aβ levels have previously been reported to fluctuate over time [19], we found
295 that ISF ILEI levels tended to inversely fluctuate relative to the fluctuating levels of Aβ (Fig. 3E, F).

296

297 *Activity-dependent release of ILEI and Aβ*

298 Using reverse microdialysis, we tested pharmacological modulation of synaptic activity.
299 Preliminary reverse microdialysis of bromophenol blue solution in the frontal cortex resulted in its focal
300 diffusion within the restricted area even after continuous perfusion for 48 h (Fig. 4A). Perfusion with
301 tetrodotoxin, a voltage-dependent sodium channel blocker, suppressed ILEI levels in a dose-dependent
302 manner (Fig. 4B). A similar decrease in ISF Aβ levels was reported in a previous report [12].
303 Intraperitoneal administration of tetanus toxin, an inhibitor of synaptic vesicle exocytosis, decreased
304 ILEI and Aβ levels in the dialysates (Fig. 4C), indicating that the release of ILEI and Aβ into the ISF is
305 associated with synaptic vesicle exocytosis. Levels of ISF ILEI decreased by >95% after tetanus toxin
306 treatment, suggesting that ISF ILEI was predominantly derived from synaptic vesicles. Furthermore,
307 given that the rates of ILEI and Aβ showed similar declines after tetanus toxin treatment, the half-life of
308 ISF ILEI was apparently equivalent to that of Aβ, which has previously been reported to be as short as
309 ~2 h [20].
310
311 *Activation and inhibition of glutamatergic receptors*
312 Our finding that ISF levels of ILEI and Aβ were similarly associated with neuronal activity but
313 inversely fluctuated in untreated mice seemed paradoxical. To address this issue, we examined how
314 evoked activation or basal activity inhibition of distinct neurotransmitter receptors affected ISF ILEI and
315 Aβ levels. Hettinger et al. [21] reported that reverse dialysis of AMPA and NBQX, an agonist and
316 antagonist of AMPA-type receptors, respectively, gradually decreased ISF Aβ levels in the hippocampus

317 of mutant AβPP- and mutant Presenilin-1-double transgenic (*APPswe/PS1ΔE9*) mice. We observed
318 similar effects of AMPA and NBQX on ISF Aβ levels following cortical microdialysis in $App^{NL-G-F}$ mice
319 (Fig. 5A, B). Specifically, NBQX decreased ISF ILEI levels, whereas AMPA increased ISF ILEI levels
320 from 20 h after reverse dialysis began (Fig. 5A, B). An important characteristic of AMPA receptors is
321 rapid desensitization; in a previous study, perfusion of 1 μM and 100 μM AMPA into the rat
322 hippocampus increased and decreased the 5-HT level in dialysates, respectively [22]. Similarly, we
323 tested perfusions of 1, 20, and 100 μM AMPA and found that ILEI levels increased in a dose-dependent
324 manner (Fig. 5C); this suggests that desensitization of AMPA receptors did not affect ILEI release.
325 Hettinger et al. (2018) reported a similar result for Aβ release [21].
326 Treatment with higher doses of NMDA reduced ISF Aβ in the neocortex of $App^{NL-G-F}$ mice
327 whereas treatment with D-AP5, an NMDA receptor antagonist, markedly increased ISF Aβ levels (Fig.
328 5D), consistent with previous findings from hippocampal microdialysis of *APPswe/PS1ΔE9* transgenic
329 mice [23]. Similarly, NMDA reduced ISF ILEI levels; however, D-AP5 treatment led to a delayed
330 decrease in ILEI levels (Fig. 5E).
331
332 *Activation and inhibition of GABAergic receptors*
333 Microdialysis perfusion of diazepam and baclofen, agonists of $GABA_A$ and $GABA_B$ receptors,
334 respectively, suppressed ISF ILEI and Aβ levels, whereas perfusion of the antagonists of these receptors
335 led to a marked increase in both ILEI and Aβ levels (Fig. 6). These results are consistent with the

sustained stimulation of GABAergic receptors suppressing overall cortical neuronal activity. It must be noted, however, that the decrease in ISF ILEI levels after diazepam treatment was rapid and reached >90% at its peak, while ISF Aβ levels decreased to <50% of the baseline. These findings suggest that ILEI may be released directly from $GABA_A$ receptor-expressing neurons at their depolarization. During the perfusion, we did not observe any obvious changes in mouse behavior or awake-sleep cycles.

*Activation and inhibition of cholinergic receptors*

Perfusion of nicotine and tubocurarine, an agonist and antagonist of nicotinic acetylcholine (ACh) receptors, respectively, increased ISF Aβ levels (Fig. 7A, B). Although nicotine treatment did not alter the average levels of ISF ILEI, it did result in a higher amplitude and more regular cycle of periodic fluctuations in these levels: the amplitude was approximately 50% that of the baseline level over a ~12 h cycle (Fig. 7A). Tubocurarine treatment did not have any clear effect on ISF ILEI in the acute phase but increased ILEI levels >24 h after perfusion began (Fig. 7B). Perfusion of pilocarpine and atropine, an agonist and antagonist for muscarinic ACh receptors, respectively, decreased and increased ISF Aβ levels, respectively (Fig. 7C, D), consistent with previous findings [24, 25]. Similarly, pilocarpine decreased ILEI levels; however, atropine did not affect ILEI levels (Fig. 7C, D).

*Reduced expression of ILEI in AD brains*

Using semi-quantitative immunoblotting, we previously showed that ILEI expression levels decreased in autopsy brains of AD patients compared with those of non-demented controls and non-AD disease controls, including brains of patients with corticobasal degeneration, progressive supranuclear palsy, amyotrophic lateral sclerosis, Parkinson's disease, and dementia with Lewy bodies [10]. To measure ILEI levels in autopsied brains, we validated our ELISA method with a soluble fraction of human brains as previously described. The limits of detection and quantification were 0.24 and 0.74 ng/mL, respectively. The observed-to-expected ratios of the dilutional parallelism and spiking recovery were in the ranges of 94%–99%, and 72%–99%, respectively. The intra-assay coefficient of variation was <10%. Using ELISA, we examined ILEI levels in the same set of autopsied brains according to our previous report [10], and confirmed a significant and selective decrease in ILEI levels in AD brains (Fig. 8A). Furthermore, we measured ILEI concentrations in CSF samples of clinical subjects and found that CSF ILEI levels correlated with those of $A\beta_{40}$ and $A\beta_{42}$ and were lower in AD and MCI patients than in control patients (Fig. 8B, C).

## DISCUSSION

We quantitatively examined the extracellular release of ILEI protein in the medial prefrontal cortex of the mouse brain while also comparing ILEI levels with those of Aβ peptides. We found that ISF ILEI levels exhibited circadian fluctuation, which was similar to reports on Aβ. Our results suggested that extracellular release of these proteins was associated with neuronal activity and largely depended on

373 tetanus toxin-sensitive exocytosis of the synaptic vesicle and the circadian fluctuation of ILEI and Aβ
374 was loosely linked to mouse locomotor activity. In addition, we revealed a superimposed fluctuation in
375 which ILEI and Aβ levels were inversely altered. Perfusion of agonists or antagonists for glutamate,
376 GABA, and ACh receptors differentially altered ISF ILEI and Aβ levels, indicating that these proteins
377 are released from distinct subpopulations of presynaptic terminals. Declines in ISF ILEI and Aβ levels
378 followed inhibited depolarization of AMPA, $GABA_A$, or $GABA_B$ receptor-expressing neurons, which
379 suggests that the normal activities of these receptors directly or indirectly sustain ISF ILEI and Aβ levels
380 *in vivo*.

381 The cerebral cortex predominantly consists of two types of neurons: (1) glutamatergic
382 projection neurons reciprocally connected to the thalamus and to each other, and (2) mainly local circuit
383 GABAergic neurons [26]. The basal forebrain cholinergic system innervates the neocortex to act as a
384 slow modulator that increases the excitability of neuronal networks [27]. In the present study, reverse
385 microdialysis in the cerebral cortex resulted in focal diffusion of compounds even after prolonged
386 perfusion, and infusion of agonists or antagonists was presumed to modulate activation of the target
387 receptor-expressing neurons near the dialysis probe. Output synapses of the local circuit neurons are
388 located near the dialysis probe, whereas axon terminals of the projection neurons are far from the probe
389 but involved in the reciprocal networks. ILEI and Aβ are known to be released predominantly from
390 presynaptic terminals [28, 29]. Hence, prolonged perfusion of receptor modulators would likely have
391 both direct and indirect effects on the ISF ILEI and Aβ levels around the probe. Such indirect effects are

predicted to be mediated by the inter-regional network connections in which the probe-inserted site is involved. Nevertheless, reverse microdialysis with receptor modulators in the cerebral cortex resulted in similar effects on ISF Aβ levels as those previously reported in the hippocampus [21, 23].

AMPA receptors are expressed on the major population of synapses that mediate fast excitatory transmission in the cerebral cortex. Among the receptor modulator treatments tested in this study, AMPA treatment was unique in producing opposing effects on ISF ILEI and Aβ levels: an increase in ILEI and a decrease in Aβ. The paradoxical finding that the levels of ILEI and Aβ in the ISF are similarly associated with neuronal activity but fluctuate inversely can possibly be explained by a transition in the dominancy of AMPA receptor-mediated synaptic activation. On the other hand, continuous stimulation of nicotinic ACh receptors enhanced the spontaneous fluctuation of ISF ILEI levels: nicotine treatment resulted in a higher amplitude and more regular cycle of periodic fluctuations in ILEI levels. Nicotinic cholinergic stimulation is known to potentiate glutamatergic transmission [30] and is required for the generation of synchronized ultraslow fluctuation of neuronal activity in the prefrontal cortex [31]. However, the underlying mechanism of these effects could not be addressed in the present study and it will therefore require further investigation in future research.

Recently, Rice et al. [32] reported that the distribution of AβPP is prominent in GABAergic interneurons in the hippocampus, and they showed that 98% of AβPP-positive cells in the CA1 region are $GABA_B$ receptor subunit 1-positive. In the present study, treatment with agonists of $GABA_A$ or $GABA_B$ receptors reduced ISF Aβ levels whereas treatment with antagonists of these receptors

411 remarkably increased ISF Aβ levels. While our results seem to be discordant with the findings of [32], it
412 is currently unclear whether this discrepancy is due to differences between the hippocampus and cerebral
413 cortex or between direct and indirect effects.

414 Cholinergic receptors are expressed at only 3% of the total number of nerve terminals in the rat
415 hippocampus, and AβPP is then colocalized at approximately 3%–4% of cholinergic terminals [33].
416 Nevertheless, in our study, prolonged perfusion of agonists or antagonists of these receptors led to
417 marked changes in cortical ISF levels of ILEI and Aβ. For example, nicotine perfusion unexpectedly
418 enhanced ISF Aβ levels in the cerebral neocortex. Chronic nicotine treatment has been shown to reduce
419 Aβ deposition in the brain of AβPP-transgenic (Tg2576) mice [34]. These findings suggest the
420 possibility that nicotine could produce unidentified effects on Aβ degradation or aggregation. Indeed,
421 cotinine, a stable metabolite of nicotine, can inhibit Aβ oligomerization and fibrillation [35].

422 The results of this study are consistent with those of previous studies showing that ILEI and
423 AβPP are constituents of the release-competent pool of synaptic vesicles [15, 36]. Although the
424 modulatory activities of released Aβ on synaptic transmission have been reported (reviewed by [37]),
425 the physiological functions of ILEI at the synaptic terminal remain to be clarified. Barthet, et al. [38]
426 reported that inhibiting γ-secretase cleavage of synaptic AβPP impairs the replenishment of release-
427 competent synaptic vesicles, thus, extracellular ILEI might modify these functions of Aβ and AβPP.

428 In contrast to ISF levels of ILEI and Aβ, CSF levels of these proteins were roughly paralleled
429 in mouse and clinical samples. The difference in these fluctuations between ISF and CSF may be

attributable to differences in fluid volume between ISF and CSF or in turnover dynamics between ILEI and Aβ. Our finding that CSF ILEI levels were significantly lower in AD and MCI patients than in control patients suggests that CSF ILEI might be a surrogate marker for brain Aβ accumulation or AD development. To more accurately evaluate Aβ and ILEI levels in clinical samples, it will however be necessary to carefully assess the condition of patients before and during CSF sampling.


## ACKNOWLEDGEMENTS

This research was supported by AMED under Grant Number 20dm0107141h0004 (to MNi), 20dm0107142h0004 (to TS), 20dm0107143h0004 (to TI), JP20dm0207073 (to TI), and JP18dm0107103 (to SM). This work was also supported in part by Grants-in-Aid for Scientific Research from the Ministry of Education, Culture, Sports, Science, and Technology, Japan (19K16912 to MNa, 19H03546 to MNi, and 19K21585 to MNi), and Smoking Research Foundation (to MNi).


## CONFLICT OF INTEREST

The authors have no conflict of interest to report.

## REFERENCES


[1] Chaudhury A, Hussey GS, Ray PS, Jin G, Fox PL, Howe PH (2010) TGF-β-mediated phosphorylation of hnRNP E1 induces EMT via transcript-selective translational induction of Dab2 and ILEI. *Nat Cell Biol* **12**, 286-293.

[2] Lahsnig C, Mikula M, Petz M, Zulehner G, Schneller D, van Zijl F, Huber H, Csiszar A, Beug H, Mikulits W (2009) ILEI requires oncogenic Ras for the epithelial to mesenchymal transition of hepatocytes and liver carcinoma progression. *Oncogene* **28**, 638-650.

[3] Mackenzie NC, Raz E (2006) Found in translation: A new player in EMT. *Dev Cell* **11**, 434-436.

[4] Mauri P, Scarpa A, Nascimbeni AC, Benazzi L, Parmagnani E, Mafficini A, Della Peruta M, Bassi C, Miyazaki K, Sorio C (2005) Identification of proteins released by pancreatic cancer cells by multidimensional protein identification technology: a strategy for identification of novel cancer markers. *FASEB J* **19**, 1125-1127.

[5] Waerner T, Alacakaptan M, Tamir I, Oberauer R, Gal A, Brabletz T, Schreiber M, Jechlinger M, Beug H (2006) ILEI: a cytokine essential for EMT, tumor formation, and late events in metastasis in epithelial cells. *Cancer Cell* **10**, 227-239.

[6] Maatta JA, Bendre A, Laanti M, Buki KG, Rantakari P, Tervola P, Saarimaki J, Poutanen M, Harkonen P, Vaananen K (2016) Fam3c modulates osteogenic cell differentiation and affects bone volume and cortical bone mineral density. *Bonekey Rep* **5**, 787.

[7] Bendre A, Buki KG, Maatta JA (2017) Fam3c modulates osteogenic differentiation by down-regulating Runx2. *Differentiation* **93**, 50-57.

[8] Chen Z, Ding L, Yang W, Wang J, Chen L, Chang Y, Geng B, Cui Q, Guan Y, Yang J (2017) Hepatic activation of the FAM3C-HSF1-CaM pathway attenuates hyperglycemia of obese diabetic mice. *Diabetes* **66**, 1185-1197.

[9] Chen Z, Wang J, Yang W, Chen J, Meng Y, Feng B, Chi Y, Geng B, Zhou Y, Cui Q, Yang J (2017) FAM3C activates HSF1 to suppress hepatic gluconeogenesis and attenuate hyperglycemia of type 1 diabetic mice. *Oncotarget* **8**, 106038-106049.

[10] Hasegawa H, Liu L, Tooyama I, Murayama S, Nishimura M (2014) The FAM3 superfamily member ILEI ameliorates Alzheimer's disease-like pathology by destabilizing the penultimate amyloid-β precursor. *Nat Commun* **5**, 3917.

[11] Kamenetz F, Tomita T, Hsieh H, Seabrook G, Borchelt D, Iwatsubo T, Sisodia S, Malinow R (2003) APP processing and synaptic function. *Neuron* **37**, 925-937.

[12] Cirrito JR, Yamada KA, Finn MB, Sloviter RS, Bales KR, May PC, Schoepp DD, Paul SM, Mennerick S, Holtzman DM (2005) Synaptic activity regulates interstitial fluid amyloid-β levels *in vivo*. *Neuron* **48**, 913-922.

[13] Sperling RA, Laviolette PS, O'Keefe K, O'Brien J, Rentz DM, Pihlajamaki M, Marshall G, Hyman BT, Selkoe DJ, Hedden T, Buckner RL, Becker JA, Johnson KA (2009) Amyloid

484 deposition is associated with impaired default network function in older persons without
485 dementia. *Neuron* **63**, 178-188.
486 [14] Pascoal TA, Mathotaarachchi S, Kang MS, Mohaddes S, Shin M, Park AY, Parent MJ,
487 Benedet AL, Chamoun M, Therriault J, Hwang H, Cuello AC, Misic B, Soucy JP, Aston JAD,
488 Gauthier S, Rosa-Neto P (2019) Aβ-induced vulnerability propagates via the brain's default
489 mode network. *Nat Commun* **10**, 2353.
490 [15] Liu L, Watanabe N, Akatsu H, Nishimura M (2016) Neuronal expression of ILEI/FAM3C and
491 its reduction in Alzheimer's disease. *Neuroscience* **330**, 236-246.
492 [16] Saito T, Matsuba Y, Mihira N, Takano J, Nilsson P, Itohara S, Iwata N, Saido TC (2014)
493 Single App knock-in mouse models of Alzheimer's disease. *Nat Neurosci* **17**, 661-663.
494 [17] Takeda S, Sato N, Ikimura K, Nishino H, Rakugi H, Morishita R (2011) Novel microdialysis
495 method to assess neuropeptides and large molecules in free-moving mouse. *Neuroscience* **186**,
496 110-119.
497 [18] Jansson AM, Csiszar A, Maier J, Nystrom AC, Ax E, Johansson P, Schiavone LH (2017) The
498 interleukin-like epithelial-mesenchymal transition inducer ILEI exhibits a non-interleukin-like
499 fold and is active as a domain-swapped dimer. *J Biol Chem* **292**, 15501-15511.
500 [19] Kang JE, Lim MM, Bateman RJ, Lee JJ, Smyth LP, Cirrito JR, Fujiki N, Nishino S, Holtzman
501 DM (2009) Amyloid-β dynamics are regulated by orexin and the sleep-wake cycle. *Science*
502 **326**, 1005-1007.

503 [20] Cirrito JR, May PC, O'Dell MA, Taylor JW, Parsadanian M, Cramer JW, Audia JE, Nissen JS,
504 Bales KR, Paul SM, DeMattos RB, Holtzman DM (2003) In vivo assessment of brain
505 interstitial fluid with microdialysis reveals plaque-associated changes in amyloid-β metabolism
506 and half-life. *J Neurosci* **23**, 8844-8853.
507 [21] Hettinger JC, Lee H, Bu G, Holtzman DM, Cirrito JR (2018) AMPA-ergic regulation of
508 amyloid-β levels in an Alzheimer's disease mouse model. *Mol Neurodegener* **13**, 22.
509 [22] Whitton PS, Maione S, Biggs CS, Fowler LJ (1994) Tonic desensitization of hippocampal
510 alpha-amino-3-hydroxy-5-methyl-4-isoxazolepropionic acid receptors regulates 5-
511 hydroxytryptamine release in vivo. *Neuroscience* **63**, 945-948.
512 [23] Verges DK, Restivo JL, Goebel WD, Holtzman DM, Cirrito JR (2011) Opposing synaptic
513 regulation of amyloid-β metabolism by NMDA receptors in vivo. *J Neurosci* **31**, 11328-11337.
514 [24] Beach TG, Kuo YM, Schwab C, Walker DG, Roher AE (2001) Reduction of cortical amyloid
515 β levels in guinea pig brain after systemic administration of physostigmine. *Neurosci Lett* **310**,
516 21-24.
517 [25] Caccamo A, Oddo S, Billings LM, Green KN, Martinez-Coria H, Fisher A, LaFerla FM (2006)
518 M1 receptors play a central role in modulating AD-like pathology in transgenic mice. *Neuron*
519 **49**, 671-682.
520 [26] Somogyi P, Tamas G, Lujan R, Buhl EH (1998) Salient features of synaptic organisation in the
521 cerebral cortex. *Brain Res Brain Res Rev* **26**, 113-135.

[27] Picciotto MR, Higley MJ, Mineur YS (2012) Acetylcholine as a neuromodulator: cholinergic signaling shapes nervous system function and behavior. *Neuron* **76**, 116-129.

[28] Saura CA, Chen G, Malkani S, Choi SY, Takahashi RH, Zhang D, Gouras GK, Kirkwood A, Morris RG, Shen J (2005) Conditional inactivation of presenilin 1 prevents amyloid accumulation and temporarily rescues contextual and spatial working memory impairments in amyloid precursor protein transgenic mice. *J Neurosci* **25**, 6755-6764.

[29] Willen K, Sroka A, Takahashi RH, Gouras GK (2017) Heterogeneous Association of Alzheimer's disease-linked amyloid-β and amyloid-β protein precursor with synapses. *J Alzheimers Dis* **60**, 511-524.

[30] Halff AW, Gomez-Varela D, John D, Berg DK (2014) A novel mechanism for nicotinic potentiation of glutamatergic synapses. *J Neurosci* **34**, 2051-2064.

[31] Koukouli F, Rooy M, Changeux JP, Maskos U (2016) Nicotinic receptors in mouse prefrontal cortex modulate ultraslow fluctuations related to conscious processing. *Proc Natl Acad Sci U S A* **113**, 14823-14828.

[32] Rice HC, Marcassa G, Chrysidou I, Horre K, Young-Pearse TL, Muller UC, Saito T, Saido TC, Vassar R, de Wit J, De Strooper B (2020) Contribution of GABAergic interneurons to amyloid-β plaque pathology in an APP knock-in mouse model. *Mol Neurodegener* **15**, 3.

539 [33] Rodrigues DI, Gutierres J, Pliassova A, Oliveira CR, Cunha RA, Agostinho P (2014) Synaptic
540 and sub-synaptic localization of amyloid-β protein precursor in the rat hippocampus. *J*
541 *Alzheimers Dis* **40**, 981-992.
542 [34] Nordberg A, Hellstrom-Lindahl E, Lee M, Johnson M, Mousavi M, Hall R, Perry E, Bednar I,
543 Court J (2002) Chronic nicotine treatment reduces β-amyloidosis in the brain of a mouse
544 model of Alzheimer's disease (APPsw). *J Neurochem* **81**, 655-658.
545 [35] Echeverria V, Zeitlin R, Burgess S, Patel S, Barman A, Thakur G, Mamcarz M, Wang L,
546 Sattelle DB, Kirschner DA, Mori T, Leblanc RM, Prabhakar R, Arendash GW (2011) Cotinine
547 reduces amyloid-β aggregation and improves memory in Alzheimer's disease mice. *J*
548 *Alzheimers Dis* **24**, 817-835.
549 [36] Lassek M, Weingarten J, Einsfelder U, Brendel P, Muller U, Volknandt W (2013) Amyloid
550 precursor proteins are constituents of the presynaptic active zone. *J Neurochem* **127**, 48-56.
551 [37] Ludewig S, Korte M (2016) Novel insights into the physiological function of the APP (gene)
552 family and its proteolytic fragments in synaptic plasticity. *Front Mol Neurosci* **9**, 161.
553 [38] Barthet G, Jorda-Siquier T, Rumi-Masante J, Bernadou F, Muller U, Mulle C (2018)
554 Presenilin-mediated cleavage of APP regulates synaptotagmin-7 and presynaptic plasticity. *Nat*
555 *Commun* **9**, 4780.
556
557

558 **FIGURE LEGENDS**

559 **Figure 1**

560 Characterization of mAb24C1, mAb42C1, and sandwich ELISA for ILEI. **A)** Scheme of the ILEI
561 construct and deletion mutants. The predicted conformation model of ILEI protein contains nine β-sheets
562 (β) and three α-helices (α). SS: signal sequence; V5: V5 tag. **B)** Lysates of HEK293 cells (lane 1) or
563 ILEI-knockout HEK293 cells transiently transfected with mock, V5-tagged wild-type, or various ILEI
564 deletion mutants (lanes 2–7) were subjected to SDS-PAGE. Blots were probed with anti-V5 antibody,
565 mAb24C1, or mAb42C1. **C)** Immunoblotting using lysates of ILEI-knockout HEK293 cells transiently
566 transfected with mock, V5-tagged wild-type, or various missense mutant ILEI constructs. Blots were
567 probed with anti-V5, mAb24C1, mAb42C1, or anti-GAPDH antibodies. **D)** $Gly^{169}$ and $Trp^{212}$ are distant
568 from each other on the ILEI structure: $Gly^{169}$ is located in the loop between the 2nd and 3rd α-helices,
569 whereas $Trp^{212}$ is located in the loop between the 8th and 9th β-sheets. **E)** Representative standard curves
570 from ELISA for human and mouse ILEI proteins. **F)** Immunoblotting of mouse brain lysate samples
571 with no reducing agent (nonreducing), 5% 2-mercaptoethanol (2ME), or 75 mM dithiothreitol (DTT).
572 Blots were probed using mAb24C1 or mAb42C1.

573

574 **Figure 2**

575 Extracellular levels of ILEI periodically fluctuate in the mouse brain. Brains and cerebrospinal fluid
576 (CSF) were obtained every 3 h from C57BL/6J mice that were housed under a 12:12 h light:dark cycle.

577 CSF samples from three mice at each time point were combined. ILEI levels in brain lysates **(A)**, the
578 soluble fractions of brains **(B)**, and CSF **(C)** were measured using ELISA. Aβ levels in brain lysates **(D)**,
579 the soluble fractions of brains **(E)**, and CSF **(F)** were also measured using mouse Aβ40-specific ELISA.
580 Values are shown as means ± SEMs (n = 3).
581
582 **Figure 3**
583 ISF ILEI levels are positively correlated with locomotor activity but inversely associated with ISF Aβ
584 levels. **A)** Cerebrocortical ILEI levels were monitored using *in vivo* microdialysis in a C57BL/6J mouse;
585 the movement distance of these mice was also recorded (distances moved per hour are expressed in
586 arbitrary units). A representative result is shown. **B)** Graph showing the correlation between ISF ILEI
587 levels and movement distance (n = 144, r = 0.460). **C)** Mice were intraperitoneally injected with
588 anesthetics and then with anti-anesthetic during monitoring of ISF ILEI. Values are shown as means ±
589 SEMs from three independent experiments. **D)** Cerebrocortical ISF levels of ILEI and Aβ were measured
590 after intraperitoneal injection with anesthetics. Values shown represent means ± SEM from three
591 independent experiments. All values for each mouse were normalized as percentages of the basal level,
592 which was defined as the mean concentration from samples obtained before injection (**C, D**). **E)** Cortical
593 ISF levels of ILEI and Aβ were simultaneously monitored via *in vivo* microdialysis in $App^{NL\text{-}G\text{-}F}$ mice
594 for 2 days. A representative result is shown. **F)** Reverse correlation between ISF ILEI and Aβ levels (n
595 = 112, r = 0.423).

596

597 **Figure 4**

598 ILEI is released into the ISF in a synaptic activity-dependent manner. **A)** Reverse microdialysis of
599 bromophenol blue for 48 h resulted in local diffusion in the frontal cortex of mice. The arrow indicates
600 the position of the microdialysis probe. **B)** Reverse microdialysis with tetrodotoxin (TTX) reduced the
601 cortical ISF ILEI levels of $App^{NL-G-F}$ mice in a dose-dependent manner. **C)** Intraperitoneal administration
602 of tetanus toxin decreased ISF levels of ILEI and Aβ in dialysates. Values are shown as means ± SEMs
603 from three independent experiments. All values for each mouse were normalized as percentages of the
604 basal level, which was defined as the mean concentration from samples obtained before reverse dialysis
605 or treatment.

606

607 **Figure 5**

608 Extracellular ILEI and Aβ levels were differentially altered by treatment with agonists or antagonists of
609 AMPA and NMDA receptors. Indicated doses of AMPA **(A)**, NBQX **(B)**, AMPA **(C)**, NMDA **(D)**, and
610 D-AP5 **(E)** were administered through reverse microdialysis to the frontal cortex of $App^{NL-G-F}$ mice. The
611 graphs show relative levels of extracellular ILEI (closed diamonds) and Aβ (open diamonds). All values
612 for each mouse were normalized as percentages of the basal level, which was defined as the mean
613 concentration from samples obtained before reverse dialysis.

614

**Figure 6**

Activation of $GABA_A$ or $GABA_B$ receptors reduced extracellular ILEI and Aβ levels. Indicated doses of diazepam **(A)**, picrotoxin **(B)**, baclofen **(C)**, and CGP55845 **(D)** were administered through reverse microdialysis to the frontal cortex of $App^{NL\text{-}G\text{-}F}$ mice. The graphs show relative levels of extracellular ILEI (closed diamonds) and Aβ (open diamonds). Values are shown as means ± SEMs from three independent experiments. All values for each mouse were normalized as percentages of the basal level, which was defined as the mean concentration from samples obtained before reverse dialysis.

**Figure 7**

Extracellular ILEI and Aβ levels were differentially altered by treatment with agonists or antagonists of nicotinic and muscarinic ACh receptors. Indicated doses of nicotine **(A)**, tubocurarine **(B)**, pilocarpine **(C)**, and atropine **(D)** were administered through reverse microdialysis to the frontal cortex of $App^{NL\text{-}G\text{-}F}$ mice. The graphs show relative levels of extracellular ILEI (closed diamonds) and Aβ (open diamonds). Values are shown as means ± SEMs from three independent experiments. All values for each mouse were normalized as percentages of the basal level, which was defined as the mean concentration from samples obtained before reverse dialysis.

**Figure 8**

633 Reduced expression of ILEI in the AD brain. **A)** ILEI levels in soluble fractions from temporal cortex
634 homogenates from AD brains (n = 15), age-matched non-neurological disease controls (n = 15), and
635 non-AD neurological disease controls (n = 10) were measured using ELISA. Non-AD disease controls
636 included corticobasal degeneration (2 cases), progressive supranuclear palsy (2 cases), amyotrophic
637 lateral sclerosis (2 cases), Parkinson's disease (2 cases), and dementia with Lewy bodies (2 cases). Lines
638 and error bars represent means ± SEM. Statistical analysis was performed using Dunnett's multiple
639 comparison test. Significant differences relative to the ratio in controls are indicated (mean ± SE,
640 $*p < 0.05$). **B)** ILEI concentrations in CSF from AD patients (n = 25), MCI patients (n = 25), and age-
641 matched non-neurological disease controls (n = 25) were measured using ELISA. Lines and error bars
642 represent means ± SEM. Statistical analysis was performed using Dunnett's multiple comparison test.
643 Significant differences relative to the ratio in controls are indicated (mean ± SE, $**p < 0.01$). **C)** CSF
644 ILEI concentrations were correlated with those of $A\beta_{40}$ (n = 75, r = 0.678) and $A\beta_{42}$ (n = 75, r = 0.627).
645

Figure 1

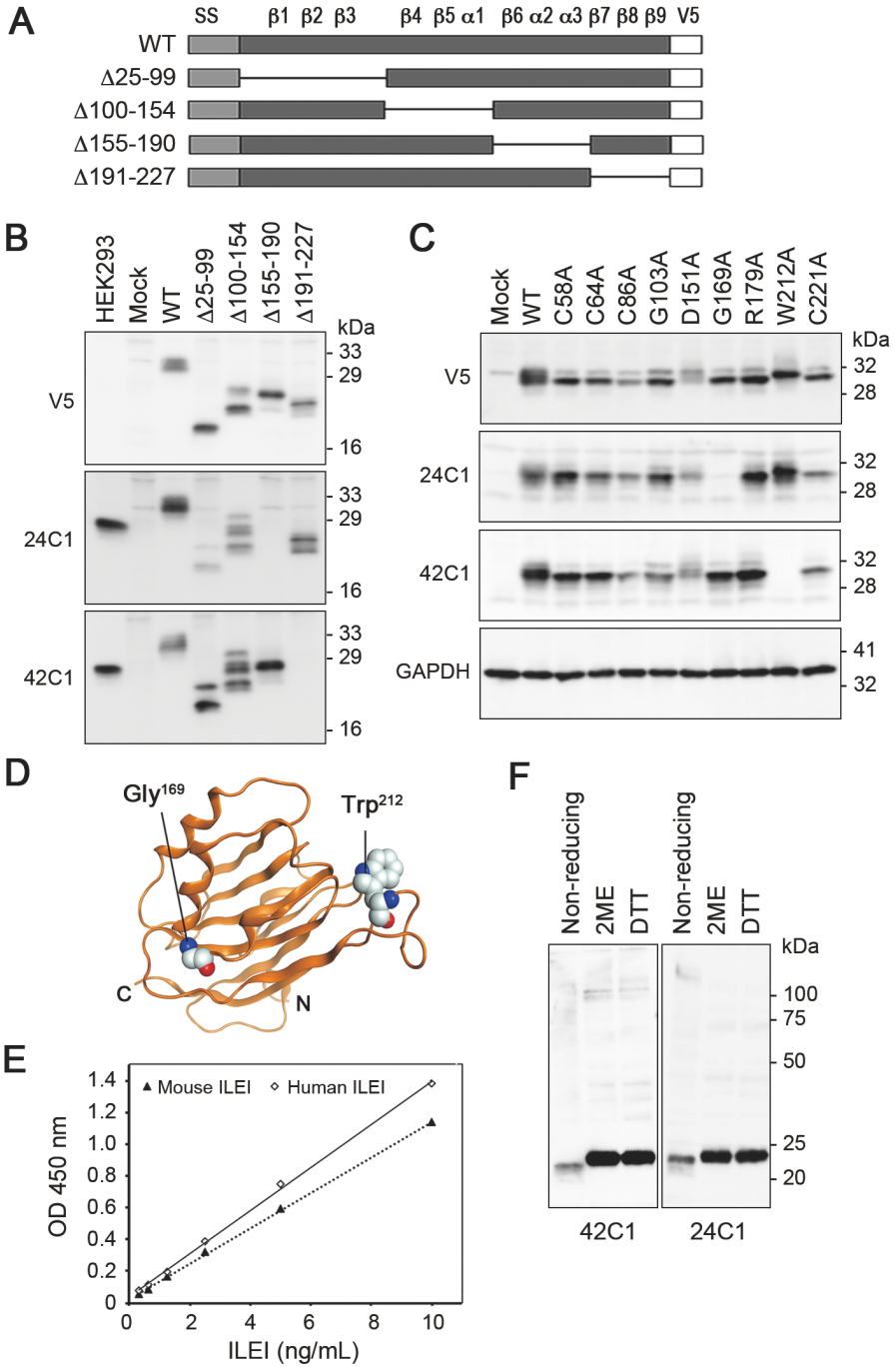
A
SS β1 β2 β3 β4 β5 α1 β6 α2 α3 β7 β8 β9 V5
WT
Δ25-99
Δ100-154
Δ155-190
Δ191-227
B
HEK293
Mock
WT
Δ25-99
Δ100-154
Δ155-190
Δ191-227
kDa
V5
24C1
42C1
33
29
16
C
Mock
WT
C58A
C64A
C86A
G103A
D151A
G169A
R179A
W212A
C221A
kDa
V5
24C1
42C1
GAPDH
32
28
41
D
Gly169
Trp212
C
N
E
Mouse ILEI
Human ILEI
OD 450 nm
ILEI (ng/mL)
F
Non-reducing
2ME
DTT
kDa
100
75
50
25
20
42C1
24C1

Figure 2

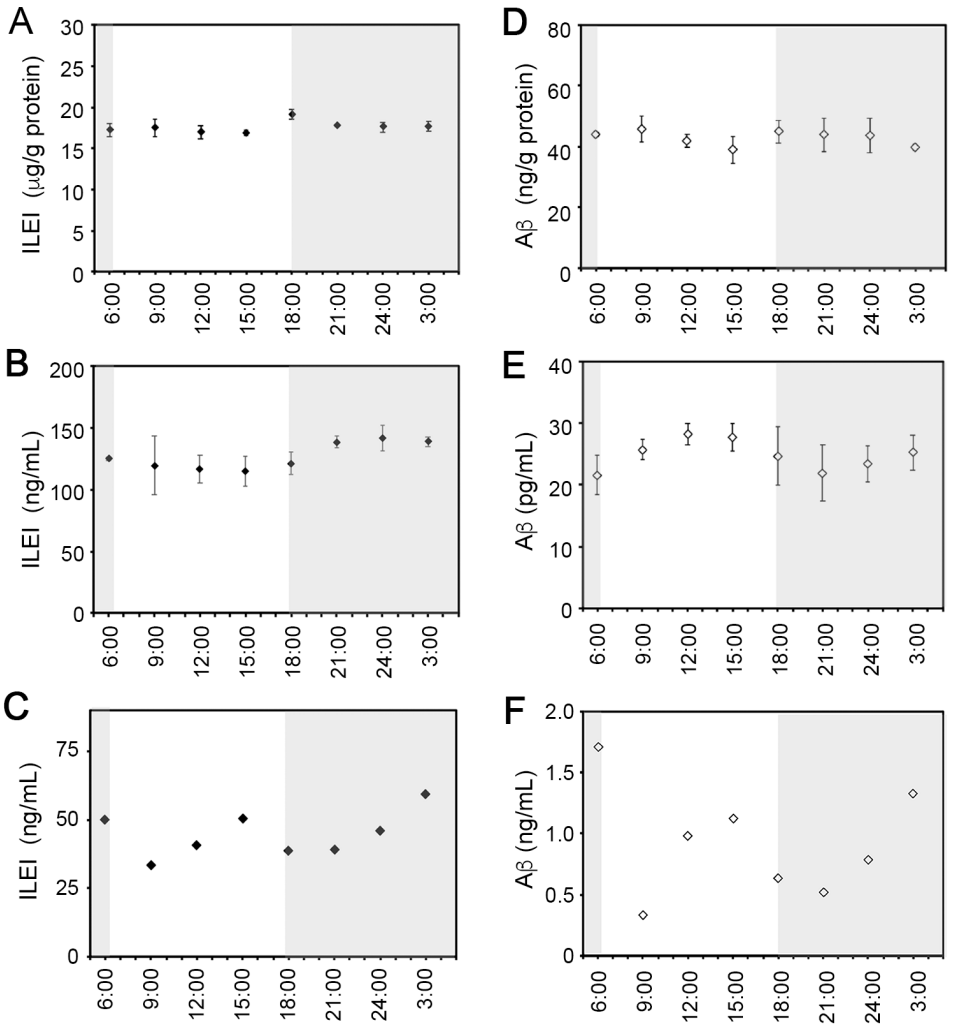
A
ILEI (μg/g protein)
30
25
20
15
10
5
0
6:00
9:00
12:00
15:00
18:00
21:00
24:00
3:00
D
Aβ (ng/g protein)
80
60
40
20
0
B
ILEI (ng/mL)
200
150
100
50
0
E
Aβ (pg/mL)
40
30
20
10
0
C
ILEI (ng/mL)
75
50
25
0
F
Aβ (ng/mL)
2.0
1.5
1.0
0.5
0

Figure 3

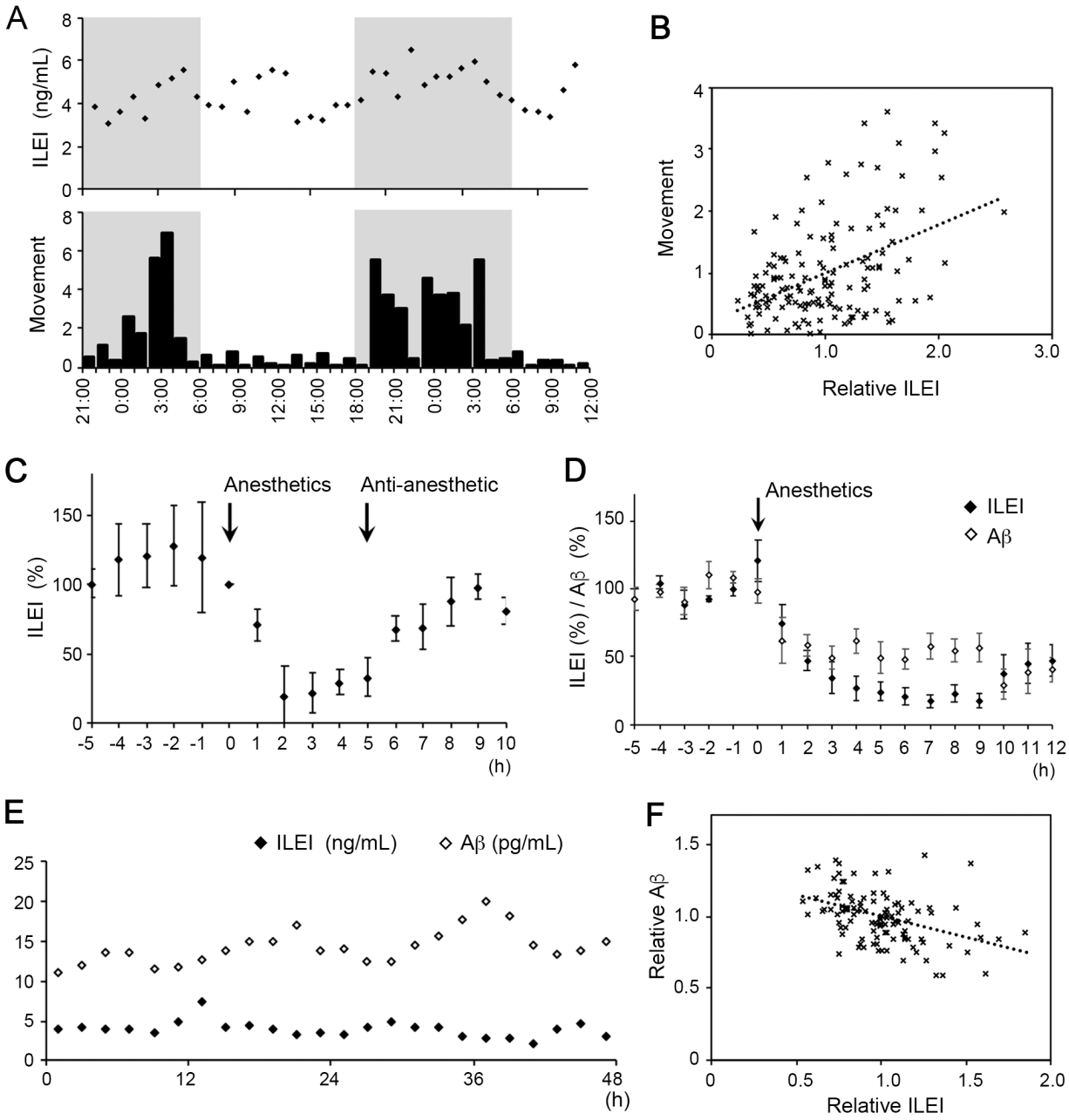
A
ILEI (ng/mL)
Movement
21:00
0:00
3:00
6:00
9:00
12:00
15:00
18:00
B
Movement
Relative ILEI
C
Anesthetics
Anti-anesthetic
ILEI (%)
(h)
D
Anesthetics
ILEI
Aβ
ILEI (%) / Aβ (%)
(h)
E
ILEI (ng/mL)
Aβ (pg/mL)
(h)
F
Relative Aβ
Relative ILEI

Figure 4

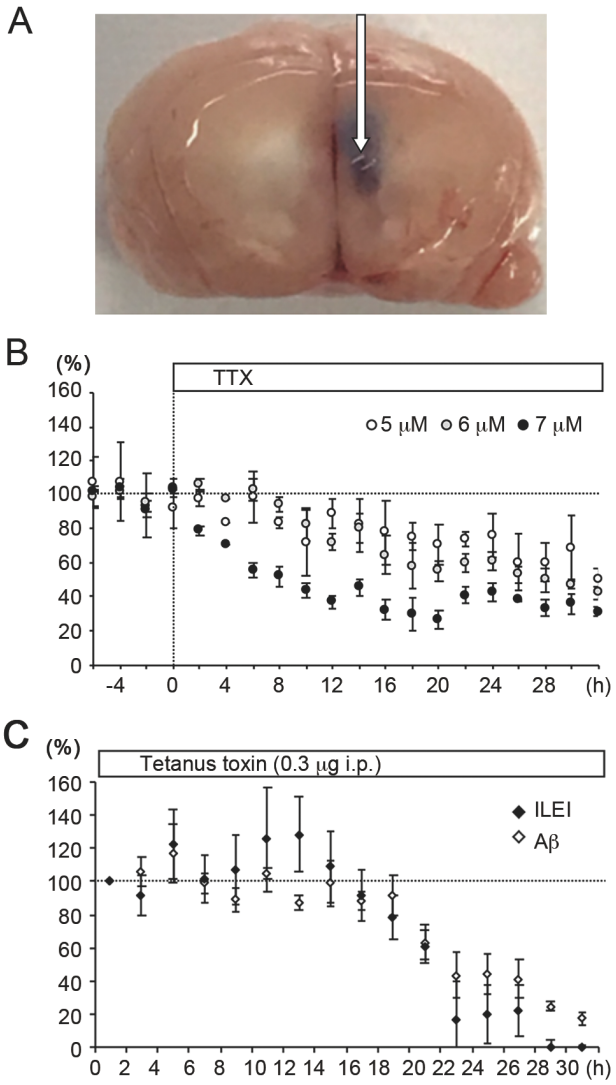
A
B
(%)
TTX
5 μM
6 μM
7 μM
160
140
120
100
80
60
40
20
0
-4
0
4
8
12
16
20
24
28
(h)
C
(%)
Tetanus toxin (0.3 μg i.p.)
ILEI
Aβ
0
2
4
6
8
10
12
14
16
18
20
22
24
26
28
30
(h)

Figure 5

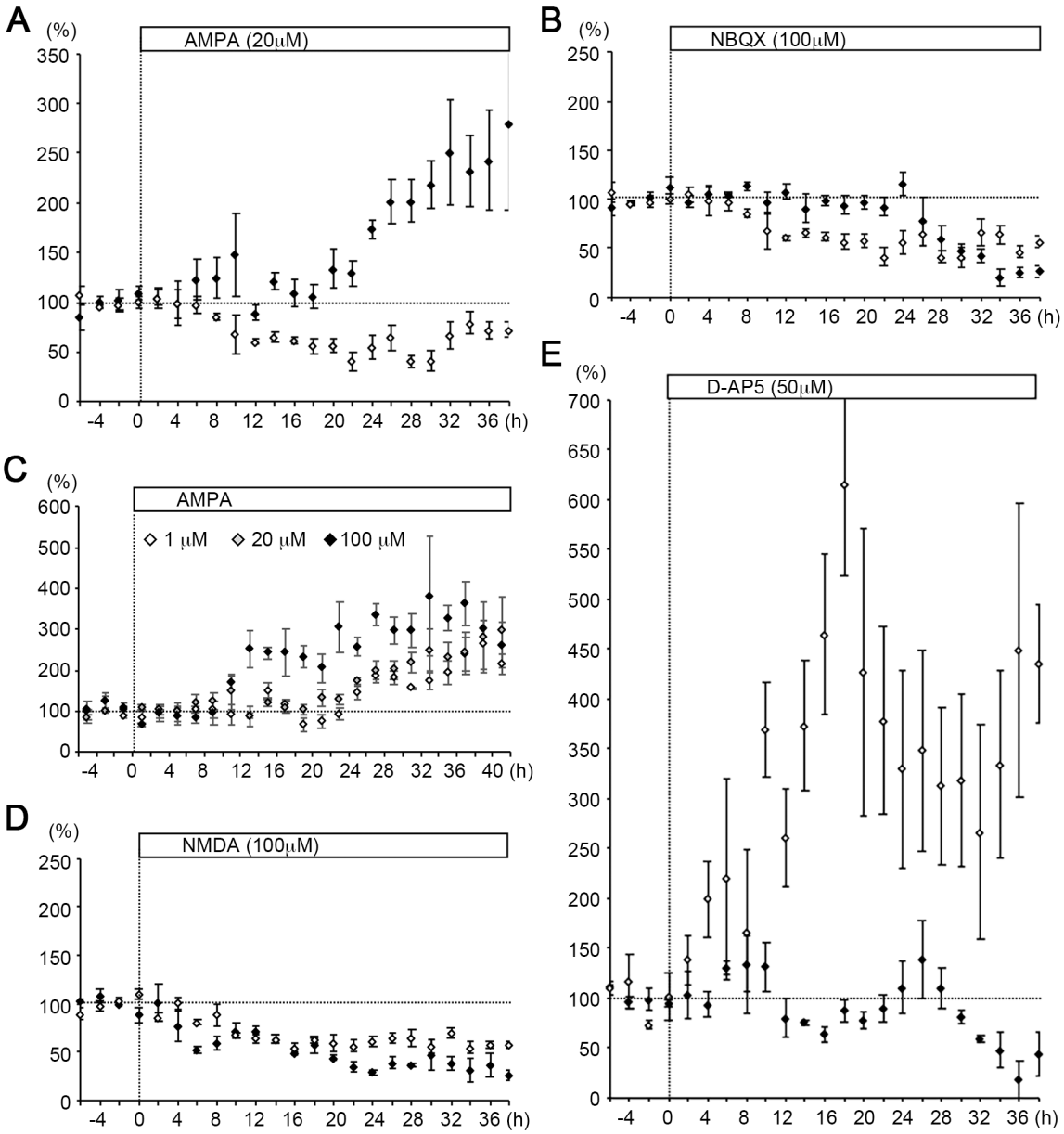
A
(%)
AMPA (20μM)
B
(%)
NBQX (100μM)
C
(%)
AMPA
1 μM
20 μM
100 μM
D
(%)
NMDA (100μM)
E
(%)
D-AP5 (50μM)
(h)

Figure 6

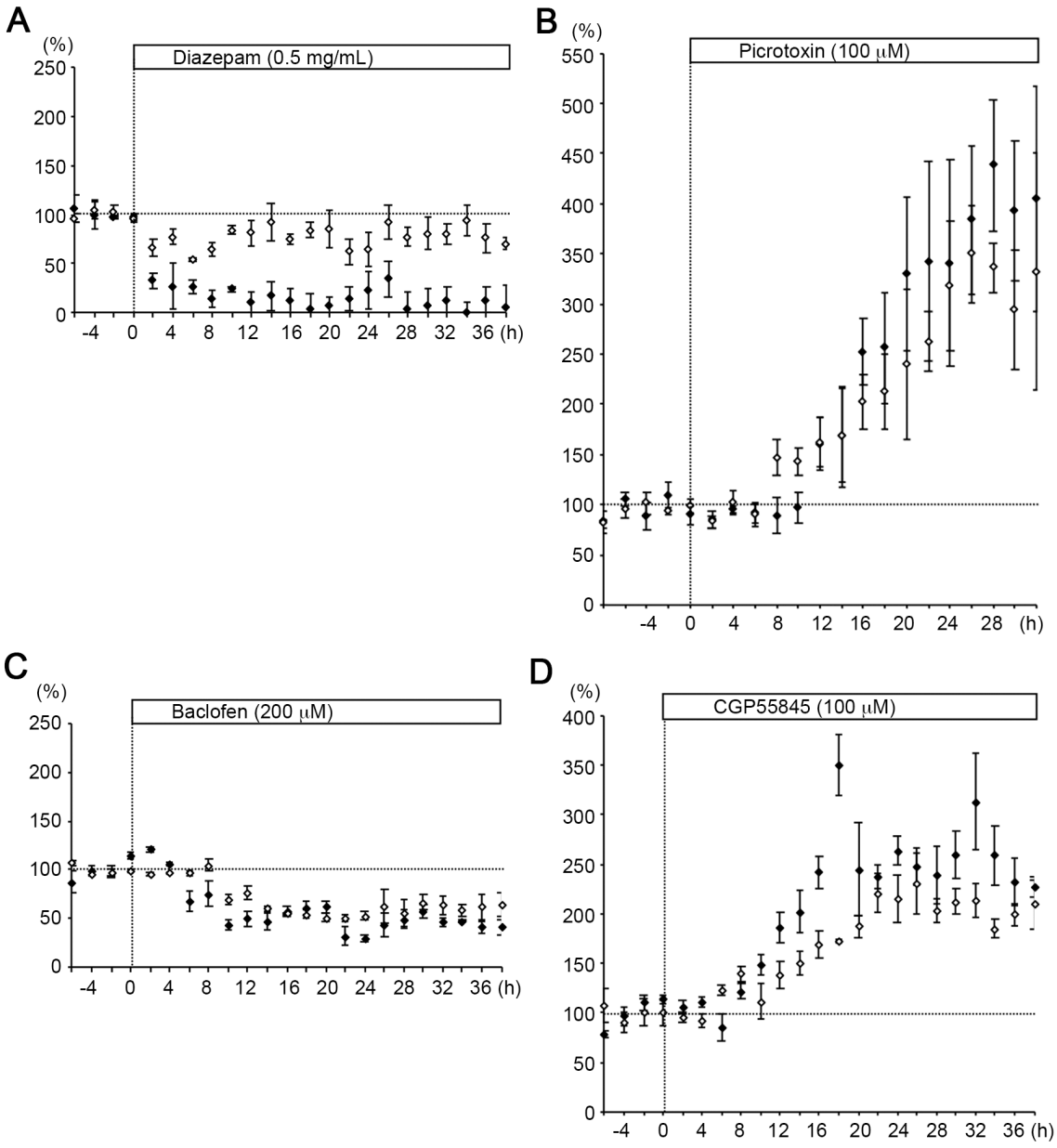
A
(%)
Diazepam (0.5 mg/mL)
250
200
150
100
50
0
-4 0 4 8 12 16 20 24 28 32 36 (h)
B
(%)
Picrotoxin (100 μM)
550
500
450
400
350
300
250
200
150
100
50
0
-4 0 4 8 12 16 20 24 28 (h)
C
(%)
Baclofen (200 μM)
250
200
150
100
50
0
-4 0 4 8 12 16 20 24 28 32 36 (h)
D
(%)
CGP55845 (100 μM)
400
350
300
250
200
150
100
50
0
-4 0 4 8 12 16 20 24 28 32 36 (h)

Figure 7

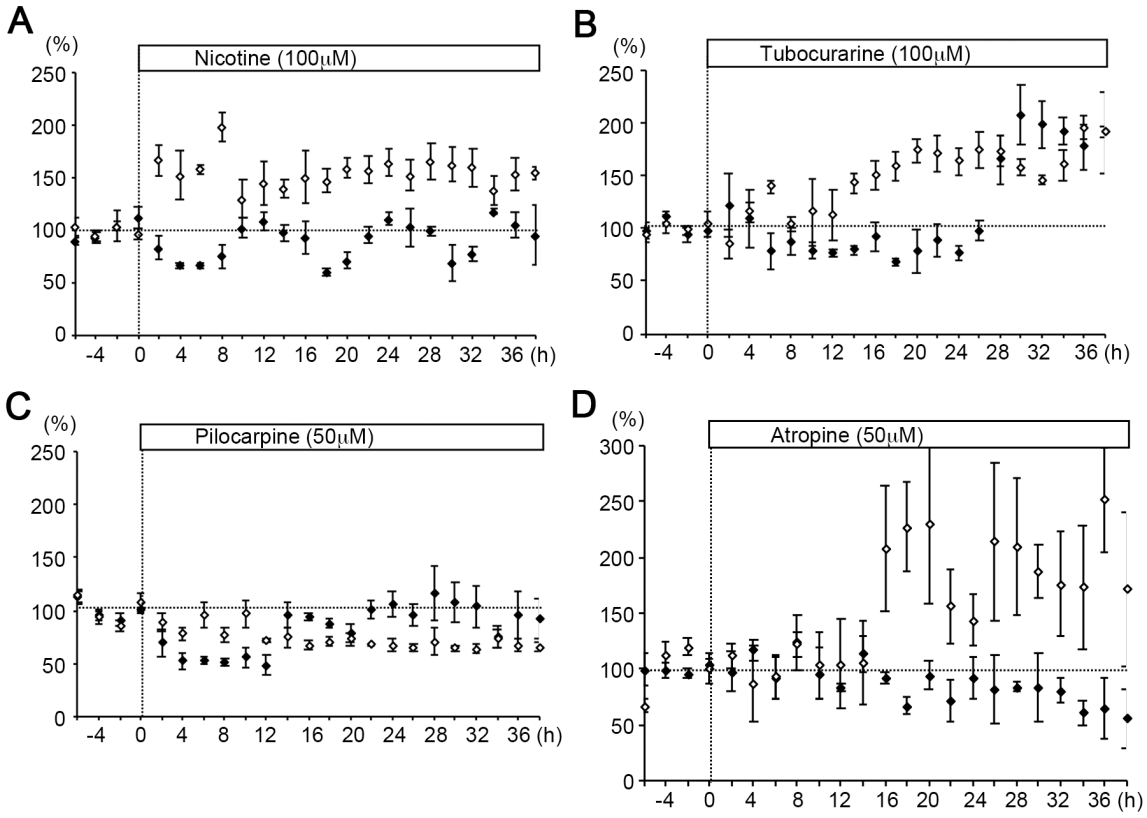
A
(%)
Nicotine (100μM)
250
200
150
100
50
0
-4 0 4 8 12 16 20 24 28 32 36 (h)
B
(%)
Tubocurarine (100μM)
250
200
150
100
50
0
-4 0 4 8 12 16 20 24 28 32 36 (h)
C
(%)
Pilocarpine (50μM)
250
200
150
100
50
0
-4 0 4 8 12 16 20 24 28 32 36 (h)
D
(%)
Atropine (50μM)
300
250
200
150
100
50
0
-4 0 4 8 12 16 20 24 28 32 36 (h)

Figure 8

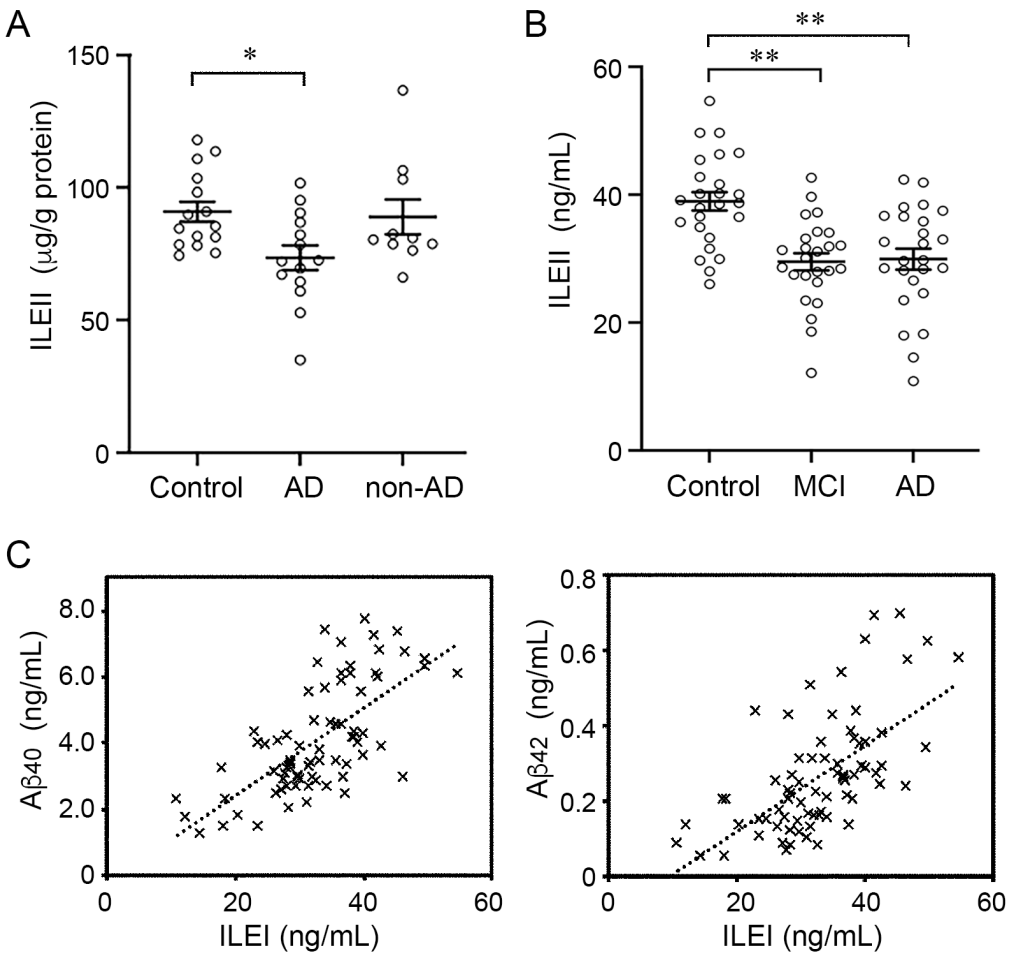
A
150
100
50
0
ILEII (μg/g protein)
*
Control
AD
non-AD
B
60
40
20
0
ILEII (ng/mL)
**
**
Control
MCI
AD
C
8.0
6.0
4.0
2.0
0
Aβ40 (ng/mL)
0
20
40
60
ILEI (ng/mL)
0.8
0.6
0.4
0.2
0
Aβ42 (ng/mL)
0
20
40
60
ILEI (ng/mL)